
Real-time Tropical Cyclone Intensity Estimation by Handling Temporally Heterogeneous Satellite Data

Anonymous Author(s)

Affiliation

Address

email

Abstract

Analyzing big geophysical observational data collected by multiple advanced sensors on various satellite platforms promotes our understanding of the geophysical system. For instance, convolutional neural networks (CNN) have achieved great success in estimating tropical cyclone (TC) intensity based on satellite data with fixed temporal frequency (e.g., 3 h). However, to achieve more timely (under 30 min) and accurate TC intensity estimates, a deep learning model is demanded to handle temporally-heterogeneous satellite observations. Specifically, infrared (IR1) and water vapor (WV) images are available under every 15 minutes, while passive microwave rain rate (PMW) is available for about every 3 hours. Meanwhile, the visible (VIS) channel is severely affected by noise and sunlight intensity, making it difficult to be utilized. Therefore, we propose a novel framework that combines generative adversarial network (GAN) with CNN. The model utilizes all data, including VIS and PMW information, during the training phase and eventually uses only the high-frequent IR1 and WV data for providing intensity estimates during the predicting phase. Experimental results demonstrate that the hybrid GAN-CNN framework achieves comparable precision to the state-of-the-art models, while possessing the capability of increasing the maximum estimation frequency from 3 hours to less than 15 minutes. *Github link for the paper will be provided.*

1 Introduction

Tropical cyclone (TC) is a type of low-pressure weather systems form and develop on the warm tropical ocean. It is characterized by intense rotating winds and severe rainfall associated with eyewall clouds and spiral rainbands. A TC hitting the land poses severe threats to society by producing gusty wind, sea surge, flooding, and landslide.

TC intensity (i.e., the maximum sustained surface wind near the center) is one of the most critical factors in disaster management. The state-of-the-art SATCON [1], widely used in operational forecasting, estimates TC intensity based on consensus decision-making procedures using infrared images from geostationary satellites and other observation from low-Earth-orbit satellites. Note that high quality SATCON estimates could be obtained with an approximate three-hour frequency.

Recently, several studies have applied convolutional neural networks (CNN) on satellite images to estimate TC intensity [2, 3, 4, 5]. The previous work released a benchmark dataset "TCIR" for the TC-image-to-intensity regression task [3], which consists of satellite images including four channels (Figure 1 (a)-(d)). The CNN-TC network[4]¹ utilized IR1 (Infrared) and PMW (passive microwave rain rates) channels and achieved the state-of-the-art performance with also a three-hour frequency.

¹This article is published in *Weather and Forecasting*, one of the best journals in the relevant research field.

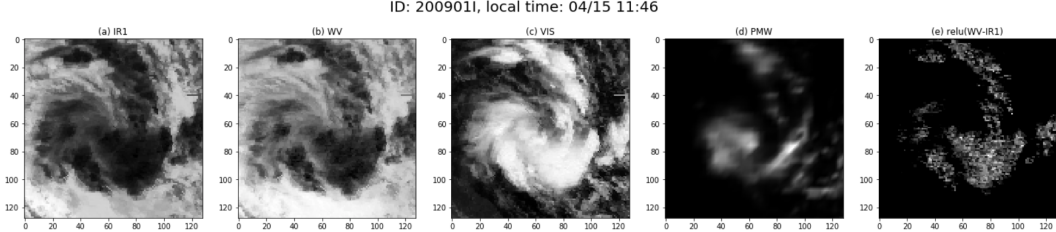


Figure 1: Channels of the TCIR dataset. (a)-(d) The four basic channels: IR1, WV, VIS, and PMW. (e) $\text{relu}(\text{WV} - \text{IR1})$. By comparing (d),(e), we can find the implicit correlations between the PMW and other channels.

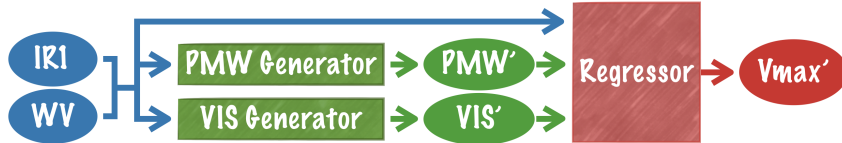


Figure 2: A schematic showing how the proposed hybrid GAN-CNN model is used for estimating TC intensity. Note that only the temporally homogeneous IR1 and WV data go into the model as the input while the GAN component generates the PMW and VIS features for the CNN regressor.

34 Notably, the VIS (visible) channel was not utilized in the past, because it only provides meaningful
 35 cloud information during the daytime. Besides, PMW channel images can only be collected at the
 36 frequency of ≈ 3 hours while the observations from IR1 and water vapor (WV) channel are available
 37 almost anytime.² As real-time intensity estimations are required for pragmatic disaster management,
 38 we must be able to handle temporally-heterogeneous satellite observations.

39 This work proposes a novel deep learning model combining CNN and GAN (generative adversarial
 40 network) to deal with the temporally heterogeneous datasets. Our goal is to eliminate the dependency
 41 on PMW channel and perform the prediction with only IR1 and WV channels, so that 24/7 intensity
 42 estimations could be provided. To keep the performance comparable to the state-of-the-art model, we
 43 also make use of the most of the information provided by good quality VIS images. We proposed
 44 a novel 5-stage training strategy, with which two separated generators are trained for producing
 45 simulated VIS and PMW images. Afterward, generated VIS and PMW images can be used along
 46 with IR1 images to conduct the estimates. Fig. 2 is a schematic of our inference model.

47 We summarize related work about GAN in Section 2 and provide analysis of various used satellite
 48 observations in Section 3. Section 4 discusses the hybrid GAN-CNN architecture and the training
 49 strategy. Then Section 5 demonstrates the capability of the proposed model dealing with temporally
 50 heterogeneous datasets to provide 24/7 intensity estimates in good quality. Section 6 is a quick recap.

51 2 Background Knowledge

52 In this section, we summarize several GAN frameworks that inspire our work. In a typical **GAN** [6],
 53 there are two opposing players: a *generator* and a *discriminator*. The generator is responsible for
 54 generating fake data and trying to confuse the discriminator. A discriminator acts like an umpire,
 55 responsible for distinguishing between real and fake data. The competition between both players
 56 prompt the generator to generate fake data that is difficult to distinguish from the real data.

57 **CGAN** (conditional GAN) [7] attaches conditions to the input of the generator. These conditions
 58 should be related to several side information provided by the image, such as the class of the object
 59 in the picture. The generator is restricted only to generate images that meet the conditions. Also,
 60 the specified conditions will be disclosed to the discriminator along with the generated data. This
 61 formulation allows generators to generate images according to our needs.

²PMW is collected by low-Earth-orbit microwave satellites. Meanwhile, IR1, WV, and VIS are collected by geostationary satellites. Normally, geostationary satellites collect data at the frequency of 15 min. In a super rapid scan mode, a geostationary satellite provides observations every 2 min.

62 **AC-GAN** (auxiliary classifier GAN) [8] follows the steps of CGAN by setting conditions to the
63 generator. Differently, specified conditions are not exposed to the discriminator. Instead, the
64 discriminator are demanded to reconstruct the side information of the images on its own. Compared
65 to CGAN, AC-GAN further improves the stability of training and the quality of the generated data.

66 In most of GAN frameworks, the discriminator only outputs a single probability to determine whether
67 the entire image is generated or not. In contrast, **PatchGAN** [9] modifies its discriminator to cut the
68 whole image into multiple small patches with overlap and discriminates them piece by piece. This
69 technique has been proven to be mathematically equivalent to doing blending with data after cutting
70 into patches. This technique is useful for data with even distribution and no distinct boundary, such
71 as satellite images.

72 **U-Net** [10] is a type of generators which has similar structure to an auto-encoder. The input and
73 output of U-Net are both images. It retains the local details from the input image by skip connections,
74 then reconstructs them in the corresponding position. Therefore, it is widely used in situations where
75 the input and output are pictures of the same size.

76 Proposed in 2017, **Pix2Pix** [11] uses pictures as the condition of the generator and completes the
77 style conversion task brilliantly. Because the inputs of the generator are images, Pix2Pix reasonably
78 uses U-Net as its generator. Meanwhile, the PatchGAN discriminator is used. L1 distance between
79 the input picture and the output picture are added to the generator loss. This term in the loss function
80 directly guides the generator to produce the desired image and is useful for fighting against *mode
collapse*. However, this framework demands data before and after conversion to be paired.

82 **CycleGAN** [12] focuses on training two generators (style A-> style B, style B-> style A) at the same
83 time instead of training an one-way generator. CycleGAN requires the input image (assuming style
84 A) can be converted back as similar as possible after passing through both generators. We can thus
85 ensure that the generator retains the critical information in the original image when converting the
86 style. The concept in CycleGAN is similar to an auto-encoder. On the other hand, CycleGAN also
87 resolves the limitation of Pix2Pix that requires the paired data. However, due to the characteristics of
88 TC images, we apply Pix2Pix in our framework, but not that of the CycleGAN. The detailed reasons
89 are described in Section 3.1.

90 3 Data Analysis and Preprocessing

91 We conducted our experiment on the benchmark TCIR dataset, which includes 4 channels: Infrared
92 (IR1), Water Vapor (WV), Visible (VIS), and Passive Microwave (PMW). An example is shown in
93 Fig. 1 (a)-(d). For more details about the TCIR, please refer to the previous work of Chen et al. [3].

94 3.1 Analysis of the PMW Data

95 According to domain knowledge, PMW is positively correlated with *relu(WV-IR1)* [13]. Therefore,
96 the Fig. 1(d) and Fig. 1(e) are somewhat similar to each other. This evidence makes us believe
97 that a properly trained Pix2Pix model can hopefully restore the PMW channel using IR1 and WV
98 information. However, since there is still a certain gap between PMW and *relu (WV-IR1)*, we cannot
99 directly use the latter one to replace the former one.

100 Besides, we also discovered that the conversion is uni-directional. While we can use IR1 and WV to
101 derive PMW, it is challenging to derive IR1 and WV from PMW. Thus, cycleGAN is not recommend
102 to serve as the PMW generator.

103 3.2 Analysis of the VIS Data

104 The VIS channel is the noisiest compared with other three channels. Types of effects includes:

- 105 1. VIS images are meaningless at night due to the significant decrease in light intensity.
- 106 2. Even under the daylight, about 1/5 of the VIS are noisy or completely black.
- 107 3. The intensity of sunlight varies at different hours throughout the day. Cloud is more obvious
108 when the time is closer to noon.
- 109 4. Similar to other channels, the signal may be disturbed by noises. Sometimes even half of a
110 VIS image is black. Besides, there could be strip noise occasionally.

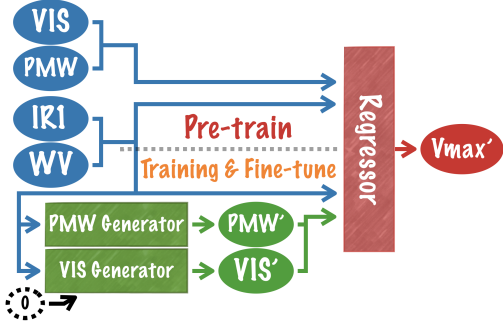


Figure 3: Framework of hybrid GAN-CNN.

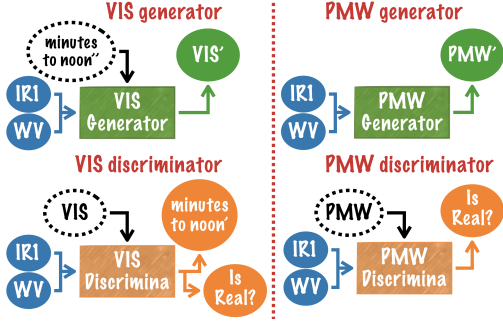


Figure 4: Illustration of two sets of GANs.

111 By adopting the VIS generator, we want to (1) generate VIS images with IR1 and WV at all times,
 112 even during the night, (2) calibrate sunlight level among all VIS images, and (3) remove block and
 113 strip noise. For clearer example, please refer to Fig. 9 in the experiment section.

114 3.3 VIS Quality Control

115 A subset of VIS data with good quality is needed to serve as the labeling data and facilitate the
 116 training of the VIS generator. This selection was conducted based on the calculation of the mean and
 117 standard deviation of the entire image values.

118 By filtering unusual values of mean, we can exclude all-black and all-white images. On the other
 119 hand, a clear VIS image's standard deviation is likely to fall within a certain interval. After consulting
 120 human experts, we subjectively determine the range of reasonable mean and standard deviation in
 121 which a high-quality VIS should be (1) $0.1 \geq \text{mean} \geq 0.7$ and (2) $0.1 \geq \text{std} \geq 0.31$.

122 Moreover, to further reduce false positives, we limit high-quality visible images to be between 07:00
 123 and 17:00 because it is impossible to have high-quality VIS data during the nighttime, namely our
 124 third condition: (3) $7 \geq \text{local_time.hour} \geq 17$.

125 As a result, a total of 12480 TC images (training data) were marked as good quality VIS, accounting
 126 for 20.9% of the total 59837 samples in the training data.

127 4 Proposed Method

128 To eliminate the dependence on the usage of PMW and solve problems caused by severe noise
 129 in the VIS, we demand GANs that can stably generate VIS and PMW channels only by the two
 130 temporally homogeneous channels: IR1 and WV (Fig. 3). In the dataset, every set of TC images have
 131 PMW observation, while only 20% have good-quality VIS. To use available information optimally,
 132 generators for PMW and VIS are trained separately (Fig. 4).

133 We use an adjusted U-Net for the **generator**. Thanks to the skip connections in U-Net, local details
 134 in the source image can be preserved. Regarding the **discriminator**, we use the idea of **PatchGAN**.
 135 Satellite observations are continuous, without concept of objects, foreground, background, and
 136 boundaries. Radically speaking, any segmentation of a real TC image can be determined normal
 137 because there is no object to be dissected. A PatchGAN divides images into multiple small areas
 138 before determining whether it is real, which is suitable for our data and makes training more stable.

139 4.1 Training Objective

140 There are three components in this framework: a generator, a discriminator, and a regressor. The loss
 141 functions are formulated as:

$$\begin{aligned}\mathcal{L}_{D_{target}} &= l_{disc} + \gamma \times l_{m2n} \times [[\text{target} = \text{vis}]] \\ \mathcal{L}_{G_{target}} &= l_{gen} + \alpha \times l_{L2} + \beta \times l_{regr} + \gamma \times l_{m2n} \times [[\text{target} = \text{vis}]] \\ \mathcal{L}_R &= l_{regr}, \quad \text{target} \in \{\text{vis}, \text{pmw}\}\end{aligned}\tag{1}$$

142 α, β, γ used in the experiments are listed in Appendix B.

143 **Discriminator loss (\mathcal{L}_D)** The goal of the discriminator is to correctly identify the target image as
 144 real observation or a fake generated by the generator:

$$l_{disc}(G, D) = \mathbb{E}_{ir1, wv, target} [\log D_{disc}(ir1, wv, target) + 1 - \log D_{disc}(ir1, wv, target')], \quad (2)$$

$$target' = G_{target}(ir1, wv), target \in \{vis, pmw\}$$

145 This concept is the same as that in the Pix2Pix.

146 **Generator loss (\mathcal{L}_G):** The loss contains the following requirements associated with our loss
 147 function. First, the goal of the generator is to confuse the discriminator:

$$l_{gen}(G, D) = \mathbb{E}_{ir1, wv, target} \log D_{disc}(ir1, wv, target'), \quad (3)$$

$$target' = G_{target}(ir1, wv), target \in \{vis, pmw\}$$

148 This is equivalent to the loss in the patchGAN.

149 Second, the generated VIS/PMW must be similar to the input VIS/PMW:

$$l_{L2}(G) = \mathbb{E}_{ir1, wv, target} ||target - target'||_2, \quad (4)$$

$$target' = G_{target}(ir1, wv), target \in \{vis, pmw\}$$

150 This concept is borrowed from the Pix2Pix. Note, however, that the L2 distance (MSE) is used instead
 151 of the L1 distance (MAE) in our model because L2 distance encourages more blurring. Usually, we
 152 want to generate images with clear lines and apparent boundaries. However, satellite images have
 153 no concept of boundaries, where they are smoother than ordinary pictures, such as dogs, cats, and
 154 cars. Therefore, we modify the Pix2Pix architecture based on our need. A comparison of using L1
 155 distance and L2 distance will be shown later in Section 5.2.

156 Besides, we have added the following two innovative designs to our GANs, specializing the GANs to
 157 complete tasks appropriately. The details are described in the following two sub-sections.

158 **Auxiliary time loss (l_{m2n}):** As mentioned in Section 3.2, we expect the VIS generator to adjust
 159 all generated VIS images to the sunlight level at noon. To achieve this goal, we need to first calculate
 160 $m2n$ (minutes to noon) for each VIS image: $m2n = |60 \times hour + minute - 60 \times 12|$. We take
 161 $m2n$ as an additional condition and apply the concept of the AC-GAN to our VIS generator and
 162 discriminator. Then loss function therefore has an extra term.

163 Discriminator:

$$l_{m2n}(D) = \mathbb{E}_{vis, m2n} ||m2n - D_{m2n}(vis)||_2 \quad (5)$$

164 Generator:

$$l_{m2n}(G, D) = \mathbb{E}_{ir1, wv} ||m2n' - D_{m2n}(vis')||_2, \quad (6)$$

$$vis' = G_{vis}(ir1, wv, m2n'), 0 \leq m2n' \leq 300$$

165 VIS images with good quality were obtained during daytime, specifically from 7:00 to 16:59 (see
 166 Section 3.3), so the largest value of minutes to noon is 300. In training, randomly generated floating-
 167 point numbers between [0, 300] are provided to the generator as condition.

168 **Regressor loss (\mathcal{L}_R):** Since our ultimate goal is to use the generated VIS / PMW channels as the
 169 regressor's inputs, the generator is requested to create useful features that can facilitate estimations.

170 The generator is first asked to generate PMW and VIS given the condition $m2n = 0$. The obtained
 171 results are provided to the regressor, along with IR1 and WV. Finally we can obtain our intensity
 172 estimation using generated VIS / PMW (e.g. lower part of Fig. 3). The precision of the prediction is
 173 also added to one of the terms of the generator loss:

$$l_{regr}(G_{vis}, G_{pmw}, R) = \mathbb{E}_{ir1, wv, vmax} ||vmax - vmax'||_2, \quad (7)$$

$$vmax' = R(ir1, wv, vis', pmw'), vis' = G_{vis}(ir1, wv, 0), pmw' = G_{pmw}(ir1, wv)$$

174 The term $vmax$ stands for the maximum wind velocity, the definition of TC intensity.

Stage	VIS/PMW used in regressor	Optimize target
Pre-train regressor	original	Regressor
Train generator	generated	Generator
Finetune regressor	generated	Regressor

Figure 5: 3-stage training.

Stage	Data used	VIS used in regressor	PMW used in regressor	Optimize target
1	Pre-train regressor	good quality VIS only	original	original Regressor
	Train VIS generator	good quality VIS only	generated	original VIS Generator
	Pre-train regressor	all data	generated	original Regressor
2	Train PMW generator	all data	generated	generated PMW Generator
	Finetune regressor	all data	generated	generated Regressor

Figure 6: The steps of the extended 5-stage training.

175 4.2 Strategy of Three-Stage Training

176 To fairly calculate l_{regr} , we need to pre-train the regressor. Therefore, a novel three-stage training
 177 illustrated in Fig. 3 and Fig. 5 is proposed.

- 178 1. **Pre-train regressor:** Pre-train the regressor with original VIS and PMW along with other
 179 regressor inputs and thereby let the regressor learns how to extract essential features from
 180 real VIS / PMW in advance.
- 181 2. **Train generator:** The generator and discriminator are optimized together. The loss men-
 182 tioned in Eq. (7) ensures that significant feature regressor is using will be generated.
- 183 3. **Fine-tune regressor:** With well-trained generator, we use the generated VIS / PMW features
 184 to fine-tune the regressor.

185 4.3 Strategy of Five-Stage Training

186 Good results are achieved through the above procedures of three-stage training. To be even better,
 187 VIS generator should be trained with only data with good quality VIS images. Meanwhile, the
 188 training process become more stable when 2 generators are only optimized when another one is fixed.

189 Therefore, based on the three-stage training described above, a more detailed five-stage training
 190 process illustrated in Fig. 6 is proposed. In the five-stage training, the first two stages of three-stage
 191 training are repeated for two loops:

- 192 1. Loop 1: Only data with good quality VIS images are used in this loop. PMW generator is
 193 fixed while we focus on optimizing VIS generator. When calculating loss in Eq. (7) we use
 194 the original PMW instead of a generated one.
- 195 2. Loop 2: All data are used. VIS generator is fixed while we pay attention to PMW generator.
- 196 3. After training both generators, regressor get fine-tuned using the generated PMW' and VIS'.

197 By applying five-stage training, we obtain the final operational predicting model (Fig. 2).

198 5 Experiments and Analysis

199 In the following section, two techniques proposed in the previous work will be explained briefly,
 200 including **auxiliary features** and **rotation-blending**. Please refer to Chen et al. [4] for more details.
 201 Next, we will compare our performance with related works which also focus on estimating TC
 202 intensity, including both operational meteorological models and deep learning techniques. Finally,
 203 we qualitatively analyze the quality of the proposed model. *Detailed model structures and hyper-*
 204 *parameters are disclosed in Appendix A and Appendix B respectively.*

205 In the experiments, we split the dataset into three parts: (1) Training data: TCs during 2000-2014, (2)
 206 Validation data: TCs during 2015 and 2016, (3) Testing data: TCs during 2017.

207 **Auxiliary Features:** In addition to the output from convolution layers, additional features are
 208 passed into the regressor. The auxiliary features are demonstrated to be helpful in improving the
 209 precision of estimation [4]. These features provide clues such as (1) day of year: stand for seasonal
 210 information, (2) local time, and the most influential one: (3) One-hot encoded region codes: region
 211 codes is in {WPAC, EPAC, CPAC, ATLN, IO, SH}, representing 6 different basins.

Table 1: The comparison between RMSEs of our proposed models and state-of-the-art models.

	no smoothing		w/ smoothing ³		input	frequency
	valid	test	valid	test		
ADT [14]			12.65		IR1	30 min ⁴
SATCON [1]			8.59		IR1, PMW ⁵	≈ 3H
CNN-TC [4]	10.38	–	8.74	8.39	IR1, PMW	≈ 3H
<i>CNN-TC</i> ⁶	10.13	10.13	8.62	8.89	IR1, PMW	≈ 3H
Proposed model	10.43	10.19	9.01	9.33	IR1, WV	<= 15 min

212 **Rotation Blending:** Considering the nature of TCs as a rotating weather system, TC data is
 213 rotation invariant. That is, rotations with respect to the center usually do not affect the estimation
 214 of the TC intensity. [3] demonstrated that the idea of using rotation for augmentation leads to a
 215 significant improvement in performance.

216 During the training phase, each image will be randomly rotated by any degree before feeding into our
 217 model. When it comes to inference, images will be rotated by evenly distributed ten angles ranged
 218 from 0 to 360 to collect 10 different estimations. Afterward, these intensity estimations are blended
 219 to obtain the final estimate.

220 5.1 Intensity Estimation Performance

221 The main task of this work is to accurately estimate the TC intensity, which is the output of our model.
 222 The unit of TC intensity is knot (kt) defined as its maximum wind speed (Vmax). The value of Vmax
 223 is usually ranged in [30, 180], and TCs with a Vmax larger than 96 kt are considered as intense TCs.

224 Table 1 compares our performance to other works. ADT (Advanced Dvorak Technique) [14] is
 225 a common used method to estimate TC intensity, which extract features from IR1 images before
 226 applying linear regression. SATCON [1] is the state-of-the-art model used by meteorologists in
 227 operational forecast. It highly rely on observations from low-Earth-orbit satellites.

228 The performance of our proposed model is comparable to the state-of-the-art model in both deep
 229 learning and meteorology, while our model can provide much more timely estimations.

230 In Fig. 7, we compare the validation MSE score over the first 100 epoch of training. The blue line
 231 represents the state-of-the-art model, which provides intensity estimates every 3 hours. The orange
 232 and green line shares same inputs, IR1 and WV, which is available every 15 min. The former is the
 233 model that directly uses them for estimations while the latter is our proposed model. In contrast, our
 234 adequately trained GAN model helps us further improve the performance of intensity estimation,
 235 bringing it closer to the state-of-the-art model. Most importantly, our proposed model can provide
 236 intensity estimates every 15 min.

237 5.2 Effectiveness of the L2 Distance

238 L2 distance is chosen instead of L1 distance in Eq. (4), which is different from a ordinary Pix2Pix
 239 framework. Comparing to commonly seen pictures, satellite observations are continuous and have
 240 smoother boundaries. As described in Section 4.1, using L2 distance encourages more blurring. In
 241 Fig. 8, we take VIS channels as examples, compare the generated results from models using L1
 242 distance and L2 distance. As shown, the model using L1 distance generates images less smoothly.

243 5.3 Qualitative Study

244 Fig. 9 shows the generated images from the proposed model. Compared with the original VIS
 245 images, the generated VIS image is slightly blurred, and the eye is not as clear as the original one.

³Simple smoothing techniques are applied here to obtain a boost in estimation precision [3, 4].

⁴They are currently providing estimations every 30 mins. But it could be <=15 min as well.

⁵SATCON depends on low-Earth-orbit satellites observations, which is somehow similar to the PMW.

⁶Our reproduction of CNN-TC. We add additional batch normalization layers in our reproduced CNN-TC, which leads to a minor improvement. The modified structure is disclosed in Table 4.

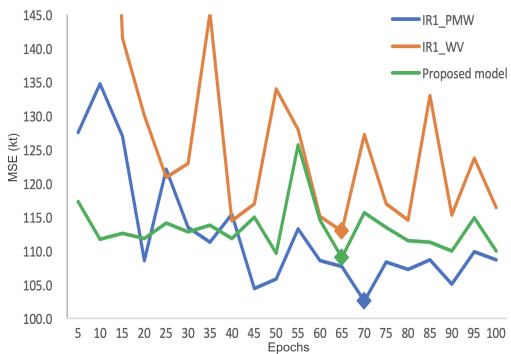


Figure 7: Learning curves in MSEs for models with different channel combinations as the input.

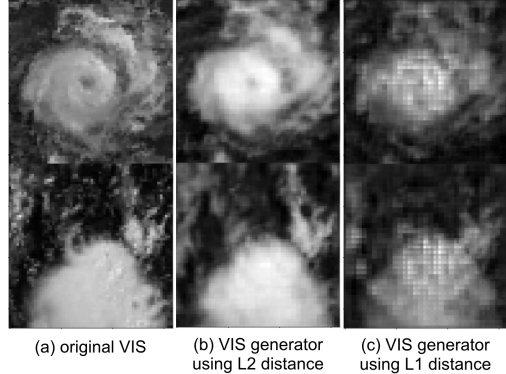


Figure 8: VIS examples generated by generators using L1 and L2 distance for l_{regr} , described in Eq. (4). Validation data is used for generating VIS in this figure.

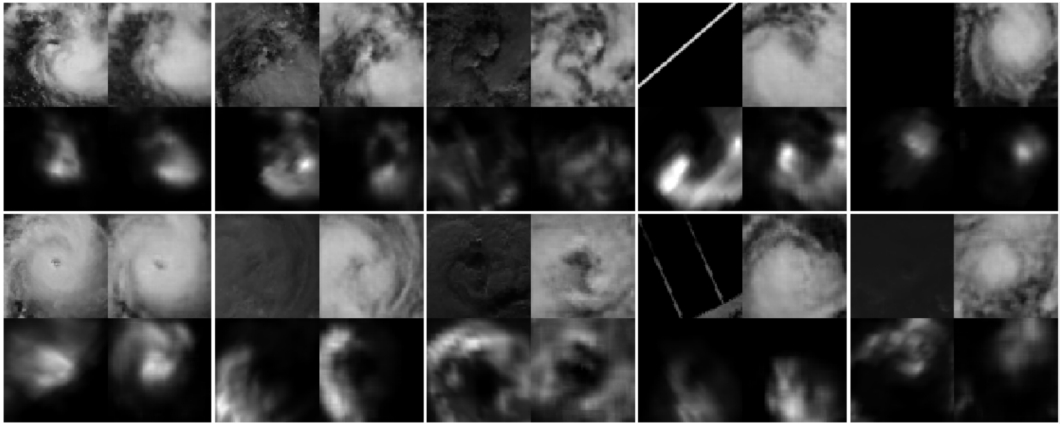


Figure 9: The generated VIS and PMW data. For each block, there are original VIS (upper left), generated VIS (upper right), original PMW (lower left), and generated PMW (lower right). Validation data is used for generating this figure.

246 Nevertheless, these images can be generated stably anytime, with the removal of most noises, and
247 with adjustment of sunlight intensity.
248 Interestingly, most of the generated PMW seems to be slightly rotated. This is presumably because
249 observations can only be obtained when the low-Earth-orbit satellites pass across the TCs. Therefore,
250 the time PMW channel being collected could be slightly misaligned with other channels.

251 6 Conclusion

252 This paper focuses on improving the utility of deep learning in TC intensity estimation for practical
253 scenarios. A modified Pix2Pix GAN framework is presented to better fit in our unusual TC data that
254 is temporally-heterogeneous, and we combine the GAN with a CNN regressor, eventually becoming
255 our proposed hybrid GAN-CNN model. By properly dealing with temporally-heterogeneous data,
256 our proposed model not only achieves comparable performance with the state-of-the-art model in
257 estimating precision but also provides the estimates much more timely, which leads to better TC
258 warning operations and could eventually save more lives.
259 Moreover, being capable of estimating TC intensity by only IR1 and WV channels, the new model
260 enables us to reanalyze the intensity of TCs further back to the time only simple IR1 and WV images
261 were available (1980s) instead of starting from 2000s, providing the potential of a breakthrough in
262 the research about climate change and global warming from the aspect of TC activities.

263 **Broader Impact**

264 Timely warnings are critical to a better disaster warning/management system. From Hurricane Katrina
265 to Hurricane Harvey and even to recent COVID-19, we should learn that early awareness of these
266 disaster could result in saving many lives.

267 Take Hurricane Harvey as example. Back to August 25, 2017, Hurricane Harvey was estimated as
268 a category 2 hurricane during 02:00 to 14:00. After it became a category 3 hurricane at 17:00, all
269 in a sudden, it grew into a category 4 hurricane only 3 hours later at 20:00. Eventually, Hurricane
270 Harvey led to the record-breaking damage in the U.S. To timely monitor this rapid intensification
271 is challenging for the conventional TC intensity estimation techniques, which provides estimates
272 only once per 3 hours. Imagine that if there's a timely estimation system which can provide intensity
273 estimates every 15 minutes. The insane increasing trend could be detected earlier, precious time
274 could be bought, people could get better prepared, and lives could be saved.

275 On the downside, a significant pitfall of applying machine learning techniques in disaster management
276 is that models are naturally conservative when facing extreme cases. For example, TC intensity
277 ranges from 20 to 180 kt, while about 70% of the value distributed within 35 kt to 64 kt, which makes
278 it almost unavoidable for machine learning models to under-estimate unprecedented extreme values.
279 Therefore, an auxiliary warning system should exist no matter how precise we humans can be with
280 our machine learning techniques. After all, disaster management is a cost-sensitive scenario in which
281 we should always keep in mind that while false positive is annoying, false negative is deadly.

282 **References**

- 283 [1] CS Velden and D Herndon. Update on the satellite consensus (satcon) algorithm for estimating
284 tc intensity. *Poster session I. San Diego*, 2014.
- 285 [2] Ritesh Pradhan, Ramazan S Aygun, Manil Maskey, Rahul Ramachandran, and Daniel J Ce-
286 cil. Tropical cyclone intensity estimation using a deep convolutional neural network. *IEEE*
287 *Transactions on Image Processing*, 27(2):692–702, 2018.
- 288 [3] Boyo Chen, Buo-Fu Chen, and Hsuan-Tien Lin. Rotation-blended cnns on a new open dataset
289 for tropical cyclone image-to-intensity regression. In *Proceedings of the 24th ACM SIGKDD*
290 *International Conference on Knowledge Discovery & Data Mining*, pages 90–99, 2018.
- 291 [4] Buo-Fu Chen, Boyo Chen, Hsuan-Tien Lin, and Russell L Elsberry. Estimating tropical cyclone
292 intensity by satellite imagery utilizing convolutional neural networks. *Weather and Forecasting*,
293 34(2):447–465, 2019.
- 294 [5] Anthony Wimmers, Christopher Velden, and Joshua H Cossuth. Using deep learning to estimate
295 tropical cyclone intensity from satellite passive microwave imagery. *Monthly Weather Review*,
296 147(6):2261–2282, 2019.
- 297 [6] Ian Goodfellow, Jean Pouget-Abadie, Mehdi Mirza, Bing Xu, David Warde-Farley, Sherjil
298 Ozair, Aaron Courville, and Yoshua Bengio. Generative adversarial nets. In *Advances in neural*
299 *information processing systems*, pages 2672–2680, 2014.
- 300 [7] Mehdi Mirza and Simon Osindero. Conditional generative adversarial nets. *arXiv preprint*
301 *arXiv:1411.1784*, 2014.
- 302 [8] Augustus Odena, Christopher Olah, and Jonathon Shlens. Conditional image synthesis with
303 auxiliary classifier gans. In *Proceedings of the 34th International Conference on Machine*
304 *Learning-Volume 70*, pages 2642–2651. JMLR.org, 2017.
- 305 [9] Chuan Li and Michael Wand. Precomputed real-time texture synthesis with markovian genera-
306 tive adversarial networks. In *European conference on computer vision*, pages 702–716. Springer,
307 2016.
- 308 [10] Olaf Ronneberger, Philipp Fischer, and Thomas Brox. U-net: Convolutional networks for
309 biomedical image segmentation. In *International Conference on Medical image computing and*
310 *computer-assisted intervention*, pages 234–241. Springer, 2015.

- 311 [11] Phillip Isola, Jun-Yan Zhu, Tinghui Zhou, and Alexei A Efros. Image-to-image translation with
312 conditional adversarial networks. In *Proceedings of the IEEE conference on computer vision*
313 and pattern recognition, pages 1125–1134, 2017.
- 314 [12] Jun-Yan Zhu, Taesung Park, Phillip Isola, and Alexei A Efros. Unpaired image-to-image
315 translation using cycle-consistent adversarial networks. In *Proceedings of the IEEE international*
316 *conference on computer vision*, pages 2223–2232, 2017.
- 317 [13] Timothy L Olander and Christopher S Velden. Tropical cyclone convection and intensity
318 analysis using differenced infrared and water vapor imagery. *Weather and forecasting*, 24(6):
319 1558–1572, 2009.
- 320 [14] Timothy L Olander and Christopher S Velden. The advanced dvorak technique: Continued
321 development of an objective scheme to estimate tropical cyclone intensity using geostationary
322 infrared satellite imagery. *Weather and Forecasting*, 22(2):287–298, 2007.